

Comparative Electrochemical Study of Ferrocene and UiO-66-NH₂ Metal–Organic Framework Modified Glassy Carbon Electrode With/Without Reduced Graphene Oxide for Sensitive Determination of Hydroxychloroquine

Abdolhamid Hatefi-Mehrjardi^{1,*}, Hamid Reza Sobhi², Amir Hossein Esmaeili³, Behzad Ahmadzadehfard⁴

^{1,2,3,4}Department of Chemistry, PayameNoor University, PO BOX19395-4697, Tehran, IRAN

Corresponding author: Abdolhamid Hatefi-Mehrjardi

Email: hhatefy@pnu.ac.ir

Received: 30 July 2024 **Accepted:** 11 September 2024

DOI: [10.30473/ijac.2026.77002.1333](https://doi.org/10.30473/ijac.2026.77002.1333)

Abstract

Hydroxychloroquine (HCQ) is a widely studied therapeutic agent that has garnered significant attention for its potential applications across a range of diseases. HCQ has since been investigated for its immunomodulatory and antiviral properties, making it a candidate in the management of autoimmune disorders as well as certain viral infections. The development of efficient electrochemical sensors for accurate HCQ measurement is crucial for clinical and pharmaceutical applications. This study presents a comprehensive comparative electrochemical investigation of glassy carbon electrode (GCE) modified with ferrocene (FC) and UiO-66-NH₂ metal–organic frameworks (MOF), with and without reduced graphene oxide (rGO), for the sensitive detection of HCQ. FC and MOF incorporated with rGO to enhance their electrochemical properties. The fabricated HCQ sensor, with three wide linear ranges (1-50 nM, 50-1000 nM, and 1-100 μM), high sensitivity (0.265 μA nM⁻¹, 0.032 μA nM⁻¹, and 0.517 μA μM⁻¹), and low detection limit (0.215 nM), was applied successfully for the analysis of real human blood serum and urine samples.

Keywords: Ferrocene, Metal–Organic Framework, Reduced Graphene Oxide, Sensitive Electrochemical Detection, Hydroxychloroquine

* Corresponding author: E-mail: hhatefy@pnu.ac.ir

1. Introduction:

Electrode modification plays a fundamental role in the development of high-performance electrochemical sensors [1–4]. The modification of the working electrode surface enhances electron transfer rates [5], prevent undesirable reactions, improve sensitivity and selectivity, reduce response time, and lower overpotential [6]. Several factors—such as the analyte's ability to exhibit favorable redox behavior, the low cost and non-toxicity of chemicals and devices, and the chosen modification method—play a critical role in guiding the design of these systems [7].

Over the past two decades, the chemistry of metal–organic frameworks (MOFs) has grown significantly [8]. While early efforts in this field focused on expanding the structural diversity of these molecule-inspired solids, recent advances have demonstrated that MOFs provide a versatile platform for innovation in organometallic chemistry [9]. Most MOFs are solids formed by combining metal ions with organic linkers containing nitrogen- or oxygen-donor atoms [10]. The synthesis of new MOFs with novel properties has opened new avenues of innovation, and their catalytic characteristics have transformed organometallic chemistry [11].

Nanotechnology has also played a crucial role in the advancing of carbon-based electrodes [12]. New modified electrodes have been fabricated using various nanoscale metals, such as metal oxides and metallic nanoparticles, as well as nanocomposites of carbon nanotubes or graphene oxide with metallic nanoparticles and polymer–metal oxide composites [13,14]. The high surface-to-volume ratio of MOFs at the nanoscale endows modified electrodes with remarkable properties, including rapid electron transfer, high sensitivity, and excellent selectivity.

To address all these factors, recent studies have focused on preparing cost-effective, eco-friendly, and high-performance modified electrodes. MOFs have emerged as key materials in the construction of new electrodes [15], while nanomaterials have contributed significantly to technological breakthroughs in recent years [16]. These materials are widely employed across numerous studies, with notable applications in electrocatalysis [17], fuel cells [18], photonic processes [19], and electroanalytical techniques [20]. Their outstanding physical and chemical properties, derived from their

nanoscale dimensions and high surface-to-volume ratios, have attracted considerable attention [21].

Carbon-based electrodes are often modified with metallic coatings, MOFs, or alternative conductive materials to improve conductivity, stability, and catalytic activity [22]. Reports indicate that carbon electrodes modified with metallic layers or MOFs, as well as solid-state stabilized electrodes, exhibit comparable performance. Moreover, the ease of preparation, low cost, and mechanical stability of MOF-modified carbon electrodes make them highly advantageous for electrochemical applications. MOFs, carbon nanostructures, and related materials can therefore be employed to construct advanced electrochemical sensors with unique properties [23].

This work integrates the systematic optimization of square wave voltammetry parameters with analytical performance evaluation and sensor validation in biological matrices, thereby creating a robust framework for HCQ detection and revealing the significant potential of rGO-based electrode modifications in advanced electrochemical sensing.

2. Experimental

2.1. Chemicals and Solutions

Phosphoric acid ($H_3 PO_4$, 85%), potassium chloride (KCl, 99.5%), sodium hydroxide (NaOH, 99%), potassium hexacyanoferrate ($K\text{Fe}(\text{CN})_6$, 99%), methanol (99.9%), Nafion (5%), 2-aminoterephthalic acid ($H_2 BDC-NH_2$), zirconium chloride ($ZrCl_4$), dimethylformamide (DMF), acetic acid, ferrocene (FC), reduced graphene oxide (rGO), and hydroxychloroquine sulfate (HCQ, 100%) were purchased from the Merck or Sigma and used with high purity and quality.

A 0.11 M phosphate buffer with constant ionic strength was prepared for use in experiments by dissolving 1.87 g of KCl and adding 170 μL of $H_3 PO_4$ in a 250 mL volumetric flask. The initial pH of the solution was 2.1, which was then adjusted to the desired values (pHs 3–10) using 0.11 M NaOH. This procedure ensured constant ionic strength across different pH values. The HCQ stock solutions were prepared from hydroxychloroquine sulfate in PBS 0.10 M, pH 7, at a concentration of 4.1 mM.

1.2.2. Synthesis of MOF ($UiO-66-NH_2$)

For the synthesis of UiO-66-NH₂, 0.154 g of ZrCl₄ and 0.12 g of H₂BDC-NH₂ were transferred into a 50 mL beaker. Then, 30 mL of DMF and 5 mL of acetic acid were added, and the mixture was sonicated for 30 minutes to achieve complete homogenization. After preparation, the solution was placed in a porcelain crucible, sealed with aluminum foil, and subjected to oven heating at 105 °C for 48 hours. The obtained nanoparticles were washed with DMF and methanol and subsequently used for electrode modification.

2.3. Instruments and Equipment

All electrochemical experiments were carried out using a modified glassy carbon electrode (GCE/FC/MOF/rGO) as the working electrode, an Ag/AgCl electrode (3.0 M KCl) as the reference electrode, and a platinum bar as the auxiliary electrode. Voltammetric experiments were performed using a potentiostat/galvanostat (Autolab 12, Eco Chemie, The Netherlands). Data acquisition and control of voltammetric experiments were conducted with NOVA 2.1.6 software. pH measurements were performed using a Metrohm 827 pH meter equipped with a combined glass electrode.

3. Results and Discussion

In this section, a glassy carbon electrode modified with MOF, ferrocene, and reduced graphene oxide (GCE/FC/MOF/rGO) was evaluated for the detection of hydroxychloroquine (HCQ) in comparison with a glassy carbon electrode modified with ferrocene and MOF (GCE/FC/MOF). The performance of these two electrodes was assessed for HCQ determination in real biological samples, including urine and blood plasma. The techniques employed included cyclic voltammetry (CV) and square wave voltammetry (SWV). Additionally, the influence of various parameters was investigated to optimize the performance of the rGO-modified electrode.

3.1. Evaluation of GCE Cleanliness by CV

Cyclic voltammetry with a 5 mM solution of K₃Fe(CN)₆ was employed to evaluate the electroactivity and cleanliness of the glassy carbon electrode surface and to determine the magnitude of the faradaic current. Analysis of the current generated from the Fe³⁺/Fe²⁺ redox reaction provided insights into electrode surface quality and electrochemical activity. For cleaning the surface of the glassy carbon (GC) electrode, a suspension of

0.05 μm alumina and ultra-fine sandpaper (P3000) was used to obtain a completely smooth and polished surface. Finally, the electrode was rinsed with double-distilled water and ethanol. Fig. 1 presents cyclic voltammograms of the GC electrode: (a) before the cleaning process and (b) after cleaning and rinsing.

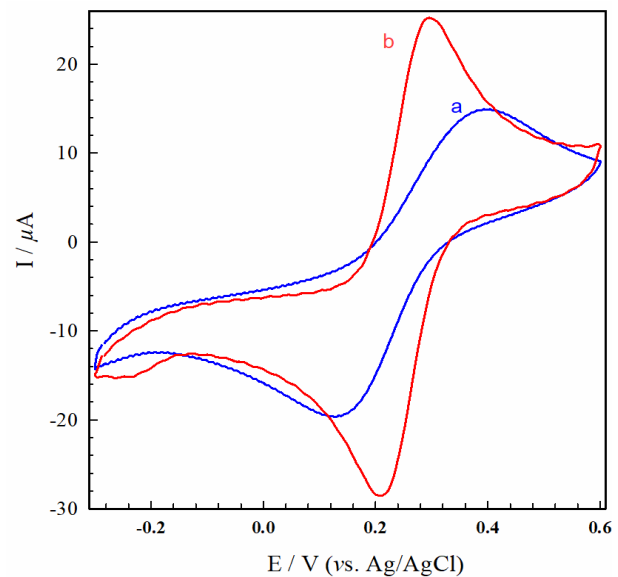


Figure 1. Comparison of cyclic voltammograms recorded at (a) the uncleaned electrode and (b) the cleaned electrode in the presence of 5 mM K₃Fe(CN)₆

It is clearly observed that prior to cleaning, the electrode surface sites were blocked, hindering electron transfer between the electrode surface and the Fe³⁺/Fe²⁺ redox couple. As a result, the peak currents decreased significantly, while the anodic and cathodic peak potentials shifted toward more positive and negative values, respectively, leading to an increased peak-to-peak separation. Consequently, the peaks became broadened and flattened. After the cleaning process, this surface blockage was removed, resulting in enhanced peak currents and reduced peak-to-peak separation, indicating that the electrode was suitably prepared for subsequent modification.

3.2 Comparison of Electrochemical Behavior of Modified GCE/FC/MOF With and Without rGO

Comparative cyclic voltammetry experiments in 0.11 M KCl solution were performed to evaluate the electrochemical behavior and performance of two modified electrodes: GCE/FC/MOF and GCE/FC/MOF/rGO. The performance of these two electrodes was compared in the presence and absence of 100 μM HCQ under various conditions. The results are shown in Fig 2.

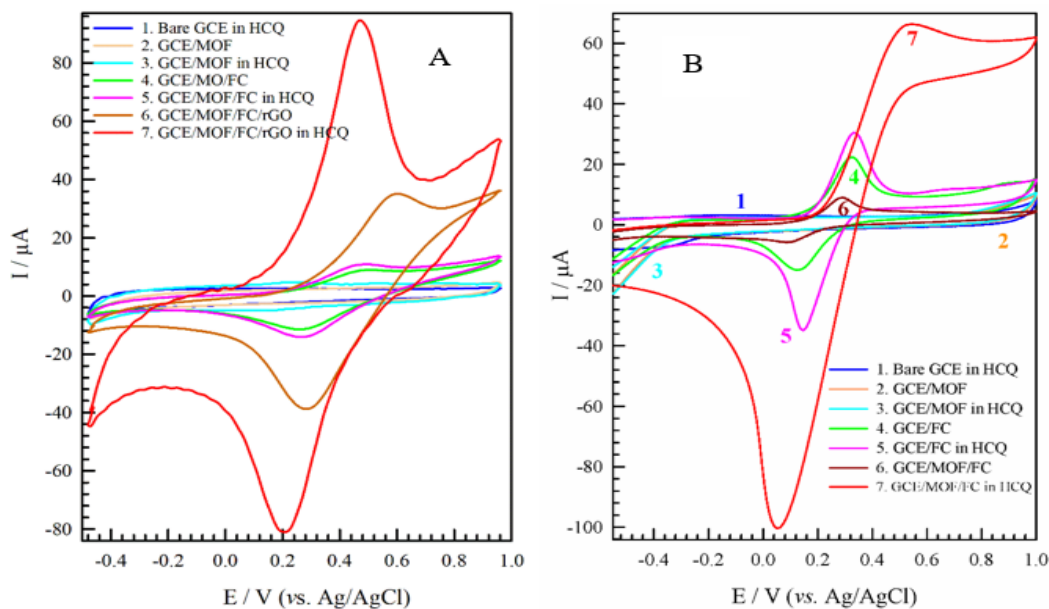


Figure 2. Comparison of CVs obtained during different stages of GCE/FC/MOF fabrication: (A) with rGO and (B) without rGO, recorded in the presence and absence of 100 μM HCQ.

Compared to the unmodified electrode (Fig. 2B), the rGO-modified electrode (Fig. 2A) demonstrates superior stability and amplified peak currents in both anodic and cathodic directions, yielding a more consistent electrochemical performance. Under equivalent experimental conditions, the incorporation of rGO into the electrode modifier was shown to favorably enhance the sensitivity of HCQ detection.

3.3 Optimization of Experimental Conditions

3.3.1 Optimization of pH by CV

The pH factor plays a significant role in electrochemical measurements. Therefore, the performance of the modified electrode must be evaluated over a range of pH. Also, to determine the optimal conditions for HCQ detection, the influence of pH on the activity of the modified electrode was evaluated. CV experiments were carried out in the absence and presence of 100 μM HCQ solution at various buffer pH values ranging from 3 to 10. The corresponding results are presented in Fig. 3.

Based on the obtained results, at pH values below 7, the rGO-modified sensor is adversely affected by the acidic conditions, leading to reduced performance. This effect is clearly evident at pH 3 (red curve). The results demonstrate that as the pH

shifts toward alkaline values, the anodic and cathodic peaks exhibit improved behavior, providing more reliable outcomes for HCQ drug detection. The optimal conditions, in terms of maximum peak current and minimum peak width at half height, were observed at pHs 8 and 9, with pH 8 showing particularly favorable characteristics. In view of the physiological pH values of blood plasma (≈ 7) and urine (≈ 6.4), and supported by comparative evaluation, pH 7 was determined to be the optimal condition. Accordingly, subsequent experiments were carried out using a buffer solution at this pH.

3.3.2 Optimization of SWV Parameters

Optimization of SWV parameters—frequency, pulse amplitude, and step potential—was carried out to achieve maximum sensitivity in HCQ detection using the modified electrode (GCE/FC/MOF/rGO). Conditions that provided the greatest peak current and the smallest half-height peak width were used to determine the optimal values. Square wave voltammograms corresponding to the optimization experiments were obtained in an electrochemical cell containing 20 mL of 0.11 M phosphate buffer (pH = 7), to which 140 μL of 100 μM HCQ solution was added.

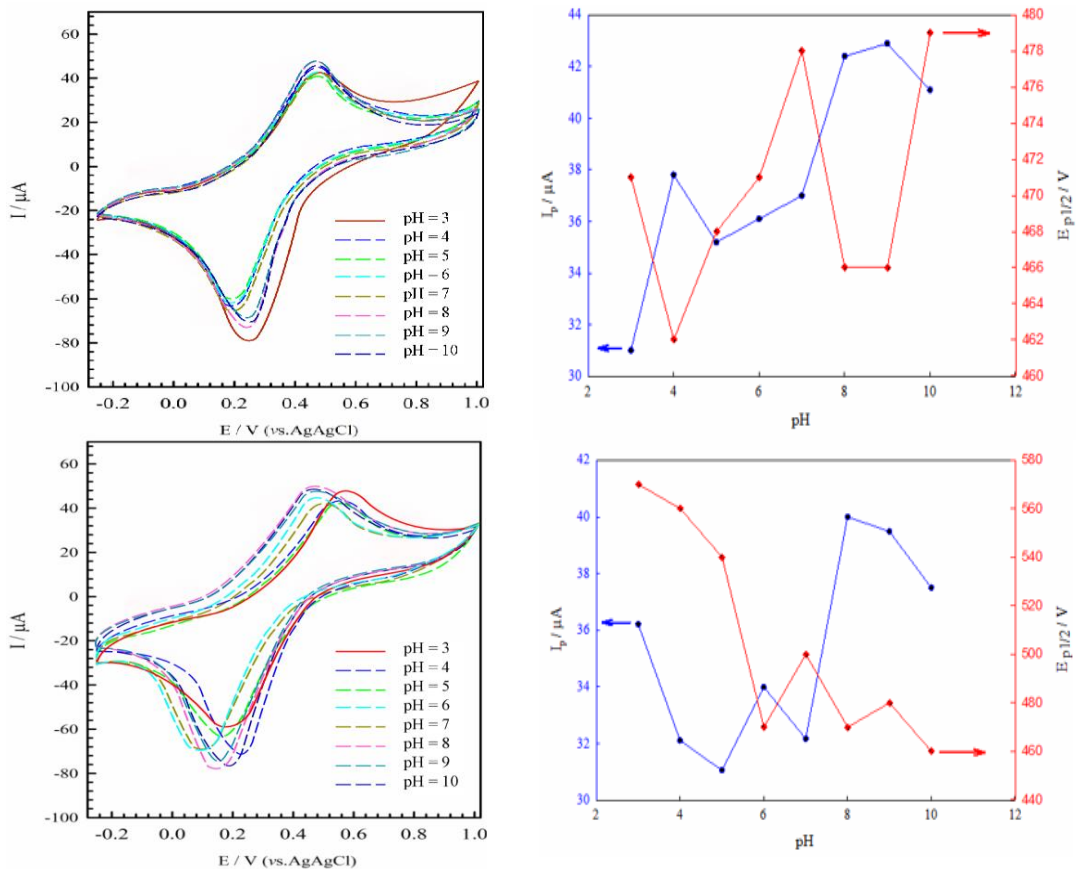


Figure 3. (left): CVs obtained from the modified electrode (GCE/FC/MOF/rGO) in the absence (top) and presence (bottom) of 100 µM HCQ in buffer solutions with varying pH values (3–10). (right): The plots of the anodic peak currents and corresponding peak potential width at half height ($E_{p,1/2}$) as a function of pH

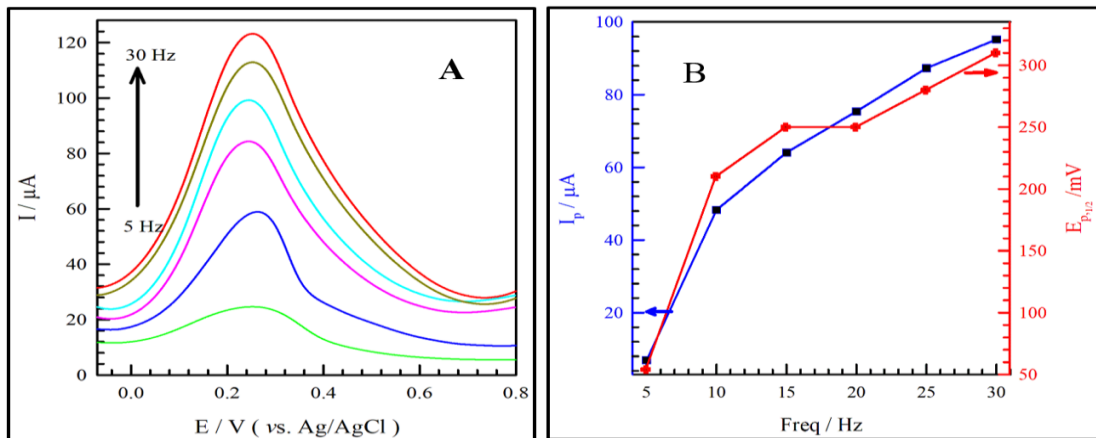


Figure 4. (A) SWVs obtained from the GCE/FC/MOF/rGO in 0.11 M PBS at pH 7 in the presence of 100 µM HCQ at different frequencies. (B) Plot of peak current and peak potential width at half height ($E_{p,1/2}$) as a function of frequency.

3.3.2.1. Optimization of Frequency

Frequency optimization was carried out by applying a 5–30 Hz range and recording square wave voltammograms of the modified electrode in HCQ solution (Fig. 4A). Quantification of anodic peak currents and half-height peak widths from the voltammograms supported the optimization study,

and analysis of plots of peak current and half-height peak potential width ($E_{p,1/2}$) versus frequency (Fig. 4B) revealed the underlying trends. The results show that although 30 Hz provided higher peak currents, the peak width was also larger that loss selectivity. Therefore, 20 Hz selected as the optimal frequency.

3.3.2.2 Optimization of Pulse Amplitude Potential

For optimization, a pulse amplitude range of 10–100 mV was applied, consistent with that used for the GCE/FC/MOF/rGO electrode (Fig. 5A). Peak currents and $E_{p,1/2}$ were quantified from the voltammograms to enable evaluation of

electrochemical trends. These trends were subsequently analyzed by constructing plots of peak currents and $E_{p,1/2}$ as a function of pulse amplitude (Fig. 5B). The results indicated that pulse amplitudes of 80 and 90 mV yielded favorable conditions; however, 80 mV was selected as the optimal pulse amplitude.

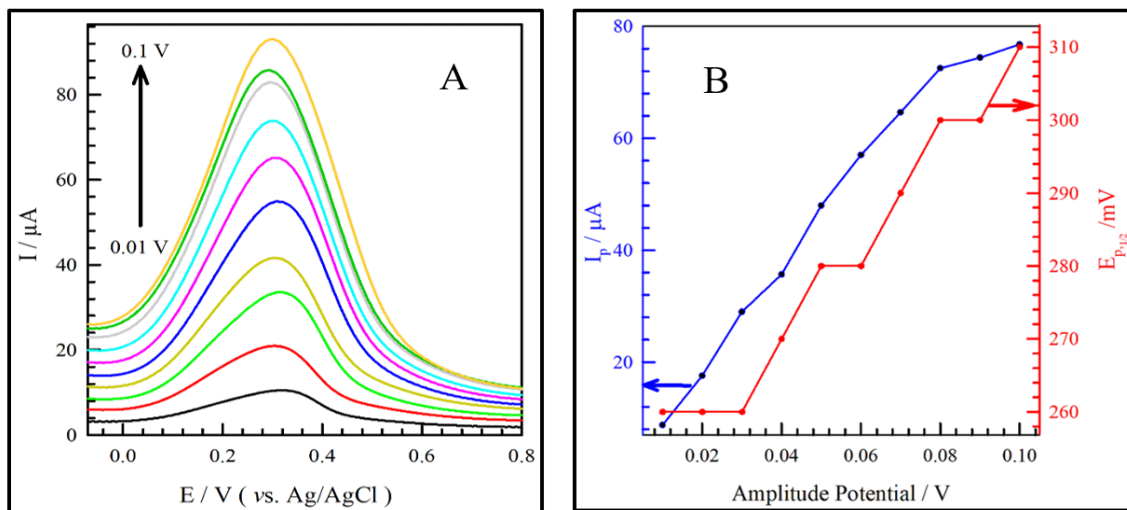


Figure 5. (A) SWVs obtained from the GCE/FC/MOF/rGO in 0.11 M PBS at pH 7 in the presence of 100 μM HCQ at different pulse amplitude potentials. (B) Plots of peak currents and $E_{p,1/2}$ as a function of pulse amplitude potentials

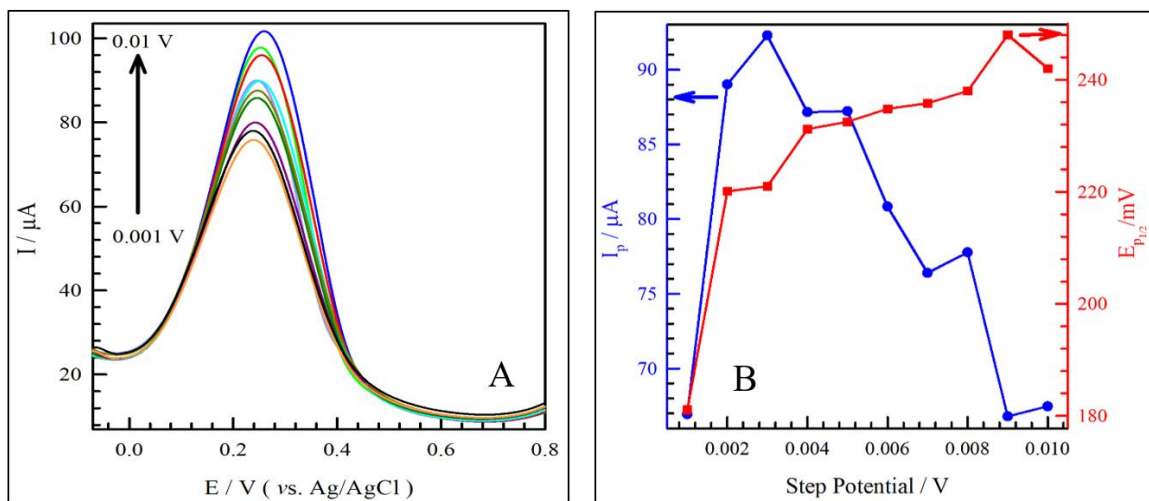


Figure 6. (A) SWVs obtained from the GCE/FC/MOF/rGO in 0.11 M PBS at pH 7 in the presence of 100 μM HCQ at different step potentials. (B) Plot of peak currents and $E_{p,1/2}$ as a function of step potentials.

3.3.2.3 Optimization of Step Potential

Precise control of electrode potential and proper timing of the electrochemical reaction require optimization of the step potential. To evaluate this effect, a step potential range of 0.001–0.01 V was applied.

(Fig. 6A). Peak currents and $E_{p,1/2}$ were extracted from the voltammograms, and trends were analyzed from plots of peak current and $E_{p,1/2}$ versus frequency (Fig. 6B), leading to the determination of 2 mV as the optimal step potential.

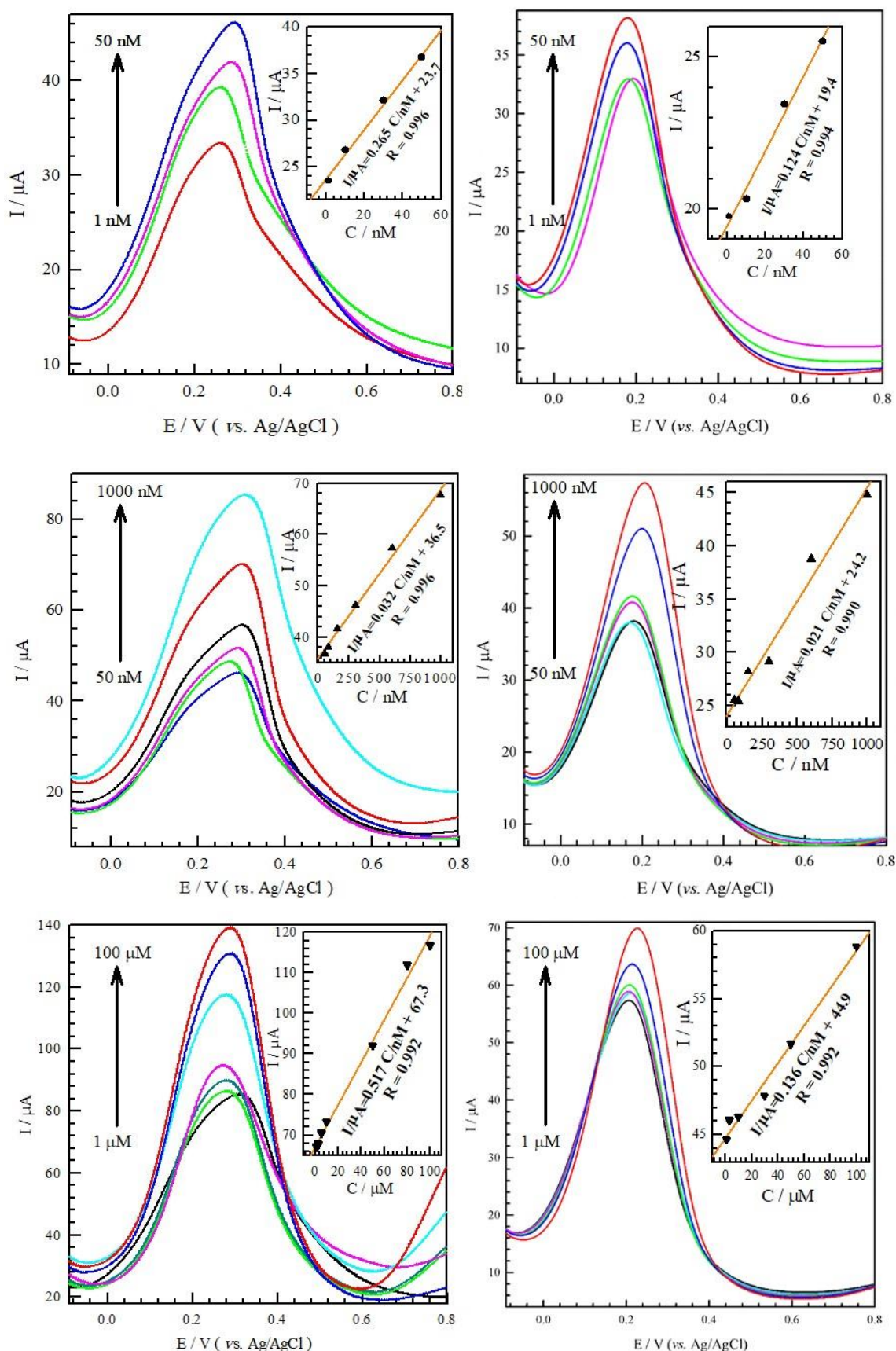


Figure 7. SWVs of the modified electrodes: (left) GCE/FC/MOF/rGO, and (right) GCE/FC/MOF, recorded over three linear ranges of HCQ concentrations. Insets show the related calibration lines and the corresponding fitted regression equations recorded within the plots.

3.4 Comparison of analytical characteristics of GCE/FC/MOF/rGO vs. GCE/FC/MOF

The electrocatalytic activity of the two modified electrodes in HCQ detection was compared under identical conditions by SWV with optimized parameters, across a concentration range of 1 nM–100 μ M. Results are presented in Fig. 7 for three concentration ranges: 1–50 nM, 50–1000 nM, and 1–100 μ M. As shown in Fig. 7 (left and right), under identical conditions and at similar concentrations, the incorporation of reduced rGO as a reinforcing agent into the GCE/FC/MOF resulted in a significant enhancement of the electrocatalytic currents. The calibration plots, along with their slopes, confirm that the GCE/FC/MOF/rGO provides greater sensitivity than the electrode without rGO.

The variations in anodic peak current as a function of HCQ concentration were plotted, and the corresponding calibration curves were presented as insets in Fig. 7 for comparison. The linear range obtained for HCQ determination (1 nM–100 μ M) under identical conditions was compared for both electrodes. Analysis of the voltammograms and corresponding calibration plots indicates that the rGO-modified electrode exhibits enhanced performance throughout the investigated concentration range. To enable a more precise comparison, the sensitivities of each modified electrode across their respective concentration ranges are summarized in Table 1.

Table 1. Sensitivities of the GCE/FC/MOF/rGO and. GCE/FC/MOF for HCQ detection extracted from Fig. 7.

Linear range	Sensitivity	
	GCE/FC/MOF/rGO	GCE/FC/MOF
1–50 nM	0.265 μ A/nM	0.124 μ A/nM
50–1000 nM	0.032 μ A/nM	0.021 μ A/nM
1–100 μ M	0.517 μ A/ μ M	0.136 μ A/ μ M

As can be seen, the slopes of the calibration lines obtained from the peak current–concentration equations for the GCE/FC/MOF/rGO are higher than those of the GCE/FC/MOF, indicating greater sensitivity. Accordingly, the GCE/FC/MOF/rGO demonstrates superior capability in detecting low concentrations of

HCQ, highlighting its improved performance compared to the GCE/FC/MOF.

The limits of detection (LOD) and limits of quantification (LOQ) for HCQ at the two modified electrode surfaces were determined by recording SWVs under identical optimized conditions in 20 mL of 0.11 M PBS, pH 7 in the absence of HCQ, with measurements repeated five times. The background currents at the oxidation peak potential of HCQ were extracted, and the relative standard deviation (S_b) was subsequently calculated. Using Eqs. 1 and 2, the LOD and LOQ values were determined:

$$\text{LOD} = 3 S_b/m \quad (\text{Eq. 1})$$

$$\text{LOQ} = 10 S_b/m \quad (\text{Eq. 2})$$

Where (m) is the slope of the calibration curve in the lowest concentration range (1–50 nM). After calculation, the LOD and LOQ values for the GCE/FC/MOF/rGO were found to be 0.215 and 0.717 nM, respectively. These values are superior to those obtained for the GCE/FC/MOF/rGO (0.255 and 0.850 nM, respectively), confirming the enhanced analytical performance of the GCE/FC/MOF/rGO.

3.5 Determination of HCQ in Real Samples

The evaluation of real samples is a fundamental aspect of clinical analysis. In this study, HCQ was determined using the modified electrode (GCE/FC/MOF/rGO) in six blood plasma samples obtained from six different individuals. One milliliter of each plasma sample, obtained from the Blood Transfusion Organization, was accurately transferred into a 100 mL volumetric flask for subsequent analysis. Also, a 10 mL aliquot of urine collected from an adult volunteer transferred into a 100 mL volumetric flask. The samples diluted with 0.11 M PBS, pH 7 to the mark. From these prepared solutions, 20 mL was taken and introduced into the electrochemical cell for analysis using SWV with the standard addition method. Each plasma or urine samples was tested in triplicate, and the results are presented in Table 2. The results confirmed the successful applicability of the proposed sensor for the determination of HCQ in real biological

samples, highlighting its potential for practical bioanalytical applications.

Table 2. Recovery test results of HCQ in real blood plasma and urine samples using GCE/FC/MOF/rGO.

Sample No.	Added (μM)	Found (μM)	Recovery (%)
Plasma			
1	1.5	1.43	95.3
2	20	20.9	104.5
3	30	28.2	94.0
4	35	36.3	103.7
5	60	58.8	98.0
6	90	88.9	98.7
Urine			
1	2.5	2.62	100.8
2	5	4.91	98.2
3	30	31.3	104.3

3.6 Comparison with other HCQ electrochemical sensors

As summarized in Table 3, the GCE/FC/MOF/rGO sensor compares favorably with recently reported HCQ sensors employing various immobilization strategies. The sensor's notable attributes include enhanced sensitivity, an ultralow detection limit, rapid response kinetics, a wide linear dynamic range, and lower overpotential.

Table 3. Comparison of some of the analytical characteristics of GCE/FC/MOF/rGO sensor with the other recently reported HCQ sensors.

Modified Electrode	Method	$E_{\text{p,a}}$ (V)	LOD (nM)	Linear range (μM)	Ref.
GCE/AuNP/f-	SWV	0.74	9.3	0.03–3.5	[24]
MWCNT				3.5–17.0	
GCE/SPCB ^a	LSV ^b	0.82	15.0	0.1–10.0	[25]
CPE/PNP/MWCNT	SWV	1.07	28	0.099–7.1	[26]
CPE/CD ^c @rGO	DPV ^d	0.53	0.0024	(1.9–3.8)×10 ⁵	[27]
CNTPE/SDS ^e	CV	0.81	850	10.0–40.0	[28]
CPE/ZnO/NprGO ^f	SWV	0.84	57	0.07–5.5	[29]
GCE/FC/MOF/rGO	SWV	0.29	0.215	0.001–0.05	This work
				0.05–1.0	
				1.00–100	

^aSuper P carbon black, ^blinear sweep voltammetry, ^ccarbon dots, ^ddifferential pulse voltammetry, ^esodium dodecyl sulphate modified carbon nanotube paste electrode, ^fZnO nanoparticles-nitrogen doped porous reduced graphene oxide

4. Conclusion

In this study, a novel electrochemical sensor based on a modified electrode (GCE/FC/MOF/rGO) was successfully developed offering sensitive and reliable determination of HCQ in biological matrices. The incorporation of rGO markedly improved the electrocatalytic activity, stability, and sensitivity of the sensor, underscoring the critical role of rGO in enhancing electron transfer and overall analytical performance. Optimization of experimental parameters—including pH, frequency, pulse amplitude, and step potential—led to enhanced analytical performance, characterized by increased peak currents and reduced peak widths.

The sensor demonstrated excellent analytical characteristics, including a wide linear range (1 nM–100 μM), low detection limit (LOD), and satisfactory limit of quantification (LOQ). Comparative studies confirmed that the GCE/FC/MOF/rGO sensor provided superior sensitivity and reproducibility, particularly at low HCQ concentrations. Furthermore, the sensor was successfully applied to real biological samples, including blood plasma and urine, thereby validating its practical utility. Recovery values approaching 100% confirmed the method's accuracy, reliability, and suitability for routine bioanalytical applications.

Overall, the proposed sensor offers a promising platform for clinical and pharmaceutical monitoring of HCQ, combining high sensitivity, reproducibility, and applicability to real samples. Its performance highlights the potential of GCE/FC/MOF/rGO in advancing electrochemical sensing technologies for drug analysis and broader biomedical applications.

Acknowledgement

The authors gratefully acknowledge Delijan Payame Noor University for supporting and providing research facilities for this work.

References

[1] N. Sandhyarani, Surface modification methods for electrochemical biosensors, in: Ali A. Ensaifi (Ed.), *Electrochemical Biosensors*, Elsevier, 2019: pp. 45–75. <https://doi.org/10.1016/B978-0-12-816491-4.00003-6>.

[2] R. Singh, R. Gupta, D. Bansal, R. Bhateria, M. Sharma, A Review on Recent Trends and Future Developments in Electrochemical Sensing, *ACS Omega* 9 (2024) 7336–7356. <https://doi.org/10.1021/AC SOMEWA.3C08060>.

[3] D.P.; Carroll, P.M. Mendes, Recent advances in surface modification and antifouling strategies for electrochemical sensing in complex biofluids, *Curr Opin Electrochem* 40 (2023) 101319. <https://doi.org/10.1016/j.coelec.2023.101319>.

[4] M. Pimpilova, A brief review on methods and materials for electrode modification: electroanalytical applications towards biologically relevant compounds, *Discov Electrochem* 1:12 (2024) 1–20. <https://doi.org/10.1007/s44373-024-00012-8>.

[5] K. Fu, J.W. Seo, V. Kesler, N. Maganzini, B.D. Wilson, M. Eisenstein, B. Murmann, H.T. Soh, Accelerated Electron Transfer in Nanostructured Electrodes Improves the Sensitivity of Electrochemical Biosensors, *Adv Sci (Weinh)* 8 (2021) e2102495. <https://doi.org/10.1002/ADVS.202102495>.

[6] M.A. Deshmukh, H.N. Thorat, N.S. Gajmal, Carbon-Based Nanomaterials in Enhancing the Performance of Electrochemical Sensors for Environmental Monitoring, in: A.M. Parambil, E. Priyadarshini, P. Rajamani (Eds.), *Carbon: Bulk-to-Nano Forms for Detection and Remediation of Environmental Contaminants*, Springer, Cham, 2025: pp. 163–187. https://doi.org/10.1007/978-3-031-90613-8_6.

[7] R.D. Crapnell, C.E. Banks, Electroanalytical Overview: Screen-Printed Electrochemical Sensing Platforms, *ChemElectroChem* 11 (2024) e202400370. <https://doi.org/10.1002/CELC.202400370>; *REQUE STEDJOURNAL:JOURNAL:21960216;ISSUE:IS SUE:DOI*.

[8] S. Kempahanumakkagari, K. Vellingiri, A. Deep, E.E. Kwon, N. Bolan, K.H. Kim, Metal–organic framework composites as electrocatalysts for electrochemical sensing applications, *Coord Chem Rev* 357 (2018) 105–129. <https://doi.org/10.1016/j.ccr.2017.11.028>.

[9] R. Lalawmpua, M. Lalhrualluangi, Lalhmunsima, D. Tiwari, Metal organic framework (MOF): Synthesis and fabrication for the application of electrochemical sensing, *Environmental Engineering Research* 29 (2024) 230636. <https://doi.org/10.4491/EER.2023.636>.

[10] Z.C. Yin, S.Q. Li, Z.Y. Shi, A. Singh, D. Srivastava, M. Muddassir, A. Kumar, J.C. Jin, New 5-nitrobenzene-1,2,3-tricarboxylate appended Cd(II) MOF: Synthesis and photoluminescent sensing of nitrofurazone (NFZ), *Mater Today Chem* 44 (2025) 102582. <https://doi.org/10.1016/J.MTCHEM.2025.102582>.

[11] R.K. Yan, X.L. Chen, J. Ren, H.L. Cui, H. Yang, J.J. Wang, Design and synthesis of a new highly efficient adjustable Ln-MOF for fluorescence sensing and information encryption, *Spectrochim Acta A Mol Biomol Spectrosc* 330 (2025) 125669. <https://doi.org/10.1016/J.SAA.2024.125669>.

[12] E. Kipkorir, O. Kimani, Electrochemical sensing of pharmaceutical pollutants using modified glassy carbon electrodes with nanostructures: A review, *Inorg Chem Commun* 179 (2025) 114827. <https://doi.org/10.1016/J.INOCHE.2025.114827>.

[13] L. Shubhadarshinee, P. Mohapatra, S. Behera, B.R. Jali, P. Mohapatra, A.K. Barick, Review on synthesis and characterization of metal nanoparticles doped carbon nanofillers based nanohybrids reinforced polyaniline nanocomposites, *Polym.-Plast. Technol. Mater* 63 (2024) 1011–1035. <https://doi.org/10.1080/25740881.2024.2314508>.

[14] A. Kumar, K.M. Gangawane, Nanoparticle-Modified Multifunctional Nano Carbons—Advances in Energy Storage, in: S.S. Kumar, P. Sharm, T. Kumar, V. Kumar (Eds.), *Advances in Sustainable Energy Technologies*, American Chemical Society, 2024: pp. 143–167. <https://doi.org/10.1021/BK-2024-1488.CH007>.

[15] T. Luan, Y. Zhao, X. Hou, Z. Tan, X. Li, J. Li, F. Wu, Integrated electrode design based on metal–organic frameworks for anion exchange membrane electrolyzers under high current densities, *J Colloid Interface Sci* 692 (2025) 137506. <https://doi.org/10.1016/J.JCIS.2025.137506>.

[16] M. Chalermnon, S.R. Thomas, J.M. Chin, M.R. Reithofer, Rational design of metal-organic frameworks (MOFs) as hosts for nanoparticles in catalytic applications: concepts, strategies, and emerging trends, *Inorg Chem Front* 12 (2025) 6435–6459. <https://doi.org/10.1039/D5QI01201E>.

[17] C. Li, H. Zhang, M. Liu, F.-F. Lang, J. Pang, X.-H. Bu, Recent progress in metal-organic frameworks (MOFs) for electrocatalysis, *Ind. Chem. Mater.* 1 (2023) 9–38. <https://doi.org/10.1039/D2IM00063F>.

[18] M.F. Sanad, S.T. Sreenivasan, Metal-organic framework in fuel cell technology: Fundamentals and application, in: S. Dave, R. Sahu, B.c. Tripathy (Eds.), *Electrochemical Applications of Metal-Organic Frameworks: Advances and Future Potential*, Elsevier, 2022: pp. 135–189. <https://doi.org/10.1016/B978-0-323-90784-2.00001-0>.

[19] H.Q. Zheng, Y. Cui, G. Qian, Guest Encapsulation in Metal–Organic Frameworks for Photonics, *Acc Mater Res* 4 (2023) 982–994. <https://doi.org/10.1021/ACCOUNTSMR.3C00169>.

[20] W. Zheng, L.Y.S. Lee, Metal–Organic Frameworks for Electrocatalysis: Catalyst or Precatalyst?, *ACS Energy Lett* 6 (2021) 2838–2843. <https://doi.org/10.1021/ACSENERGYLETT.1C01350>.

[21] C. Duan, K. Liang, Z. Zhang, J. Li, T. Chen, D. Lv, L. Li, L. Kang, K. Wang, H. Hu, H. Xi, Recent advances in the synthesis of nanoscale hierarchically porous metal–organic frameworks, *Nano Mater. Sci.* 4 (2022) 351–365. <https://doi.org/10.1016/J.NANOMS.2021.12.003>.

[22] S. Murugaiyan, M.S. Shabanur Matada, G.P. Kuppuswamy, S. Velappa Jayaraman, C. Di Natale, Y. Sivalingam, Carbon Electrodes Coated with TiO₂–Cu-MOF Composites for Nonenzymatic Detection of Ascorbic Acid, *ACS Appl Nano Mater* 8 (2025) 20164–20176. <https://doi.org/10.1021/ACSANM.5C02223>.

[23] B.M. Kim, G.W. Jang, C. Ko, K.M. Choi, W.H. Choi, J. Shin, Individually Encapsulating Metal–Organic Frameworks in Partially Reduced Graphene Oxide to Enhance Electrical Conductivity While Preserving Porosity, *ACS Appl Nano Mater* 8 (2025) 20156–20163. <https://doi.org/10.1021/ACSANM.5C02501>.

[24] N. Nardi, L.G. Baumgarten, J.P. Dreyer, E.R. Santana, J.P. Winiarski, I.C. Vieira, Nanocomposite based on green synthesis of gold nanoparticles decorated with functionalized multi-walled carbon nanotubes for the electrochemical determination of hydroxychloroquine, *J Pharm Biomed Anal* 236 (2023) 115681. <https://doi.org/10.1016/j.jpba.2023.115681>.

[25] J.P.C. Silva, D.R. Santos-Neto, C.E.C. Lopes, L.R.G. Silva, L.M.F. Dantas, I.S. da Silva, A high sensitivity adsorptive-electrochemical method for rapid and portable determination of hydroxychloroquine, *J Solid State Electrochem* 29 (2025) 1013–1023. <https://doi.org/10.1007/s10008-024-06032-z>.

[26] M.H.A. Feitosa, A.M. Santos, A. Wong, M.D.P.T. Sotomayor, W.R.P. Barros, M.R.V. Lanza, F.C. Moraes, Enhancing hydroxychloroquine detection using carbon paste electrode modified with platinum nanoparticles and MWCNTs, *J Appl Electrochem* 55 (2025) 2265–2276. <https://doi.org/10.1007/s10800-025-02293-2>.

[27] J.C. dos Santos Júnior, J. de Oliveira S. Silva, J.F. dos Santos, M.D. Santos Monteiro, M. Oliveira Rodrigues, E. Midori Sussuchi, Nanoparticles based on carbon dots and reduced graphene oxide as electrochemical sensor for voltammetric determination of hydroxychloroquine, *Electroanalysis* 36 (2024) e202300164. <https://doi.org/10.1002/elan.202300164>.

[28] P.A. Pushpanjali, J.G. Manjunatha, N. Hareesha, T. Girish, A.A. Al-Kahtani, A.M. Tighezza, N. Ataollahi, Electrocatalytic Determination of Hydroxychloroquine Using Sodium Dodecyl Sulphate Modified Carbon Nanotube Paste Electrode, *Top Catal* 68 (2025) 1373–1381. <https://doi.org/10.1007/s11244-022-01568-8>.

[29] M. Amiri, Z. Hashemi, F. Chekin, Zinc oxide nanoparticles decorated nitrogen doped porous reduced graphene oxide-based hybrid to sensitive detection of hydroxychloroquine in plasma and urine, *J Mater Sci Mater Med* 36:4 (2025) 1–11. <https://doi.org/10.1007/s10856-024-06847-2>.

مطالعه الکتروشیمیایی مقایسه‌ای الکترود کربن شیشه‌ای اصلاح شده با فروسن و چارچوب‌های فلزی-آلی

با/بدون UiO-66-NH_2 گرافن اکسید کاهش یافته برای تعیین حساس هیدروکسی کلروکین

عبدالحمید هاتفی مهرجردی*، حمیدرضا صبحی، امیرحسین اسماعیلی، بهزاد احمدزاده فرد

بخش شیمی، دانشگاه پیام نور، تهران، ایران

* E-mail: hhatefy@pnu.ac.ir

تاریخ دریافت: ۱ تیر ۱۴۰۳ | تاریخ پذیرش: ۱۶ شهریور ماه ۱۴۰۳

چکیده

هیدروکسی کلروکین (HCQ) یک عامل درمانی پر مطالعه است که توجه زیادی را به دلیل کاربردهای بالقوه آن در طیف وسیعی از بیماری‌ها به خود جلب کرده است. HCQ به دلیل خواص ایمنی تعديل کننده و ضد ویروسی مورد بررسی قرار گرفته و به عنوان گزینه‌ای در مدیریت اختلالات خودایمنی و برخی عفونت‌های ویروسی مطرح شده است. توسعه حسگرهای الکتروشیمیایی کارآمد برای اندازه گیری دقیق HCQ در کاربردهای بالینی و دارویی اهمیت فراوانی دارد. این مطالعه یک بررسی جامع و مقایسه‌ای الکتروشیمیایی از الکترود کربن شیشه‌ای (GCE) اصلاح شده با فروسن (FC) و چارچوب‌های فلزی-آلی (MOF)، با و بدون گرافن اکسید کاهش یافته (rGO)، برای آشکارسازی حساس HCQ ارائه می‌دهد. MOF همراه با rGO به منظور بهبود ویژگی‌های الکتروشیمیایی آن‌ها به کار گرفته شدند. حسگر ساخته شده برای HCQ با سه بازه خطی گسترده (۱-۵۰ نانومولار، ۵۰-۱۰۰۰ نانومولار، و ۱۰۰۰-۱ میکرومولار)، حساسیت بالا ($0.0265 \mu\text{A nM}^{-1}$ ، $0.0032 \mu\text{A nM}^{-1}$ و $0.0517 \mu\text{A \mu M}^{-1}$) و حد تشخیص پایین ($0.215 \mu\text{A nM}^{-1}$)، با موفقیت برای تعیین نمونه‌های واقعی سرم خون و ادرار انسان مورد استفاده قرار گرفت.

کلید واژه‌ها: فروسن، چارچوب فلزی-آلی، گرافن اکسید کاهش یافته، آشکارسازی الکتروشیمیایی حساس، هیدروکسی کلروکین

COPYRIGHTS



© 2022 by the authors. Lisensee PNU, Tehran, Iran. This article is an open access article distributed under the terms and conditions of the Creative Commons Attribution 4.0 International (CC BY4.0) (<http://creativecommons.org/licenses/by/4.0>)